

Heptaphosphide cluster anions bearing group 14 element amide functionalities

Gabriela Espinoza Quintero, Isabelle Paterson-Taylor, Nicholas H. Rees and Jose M.

Goicoechea*

Department of Chemistry, University of Oxford, Chemistry Research Laboratory, 12

Mansfield Road, Oxford, OX1 3TA, U.K.

Abstract. Reactions of the protonated heptaphosphide dianion, $[\text{HP}_7]^{2-}$, with one equivalent of $\text{E}[\text{N}(\text{SiMe}_3)_2]_2$ ($\text{E} = \text{Ge}, \text{Sn}, \text{Pb}$) give rise to novel derivatized cluster anions $[\text{P}_7\text{EN}(\text{SiMe}_3)_2]^{2-}$ ($\text{E} = \text{Ge}$ (**1**), Sn (**2**) and Pb (**3**)). All three species were characterized by multi-element solution-phase NMR spectroscopy and electrospray ionization mass spectrometry. In addition, **1** and **2** were structurally authenticated by means of single crystal X-ray diffraction in $[\text{K}(\text{18-crown-6})]_2[\text{P}_7\text{EN}(\text{SiMe}_3)_2] \cdot 2\text{py}$. Interestingly, while **2** appears to be indefinitely stable in solution for prolonged periods of time, the germanium-containing analogue, **1**, readily decomposes at room temperature giving rise to the dimeric species $[(\text{P}_7\text{Ge})_2\text{N}(\text{SiMe}_3)_2]^{3-}$ (**4**) and $[\text{K}(\text{18-crown-6})][\text{N}(\text{SiMe}_3)_2]$. A low quality single crystal X-ray structure of the former allowed for the confirmation of its composition and connectivity which is consistent with the ^{31}P NMR spectrum obtained for the anion.

Keywords. Zintl ions, phosphorus, polyphosphides, main-group amides.

1. Introduction

The chemistry of substituent-free group 15 Zintl anions has witnessed a renaissance over the course of the last twenty years.¹ Of the vast number of known homoatomic polynuclear anions $[\text{E}_x]^{x-}$ (where $x = 2, 5, 8$), $[\text{E}_4]^{x-}$ ($x = 2, 6$), $[\text{E}_5]^-$, $[\text{E}_6]^{4-}$, $[\text{E}_7]^{3-}$, $[\text{E}_{11}]^{3-}$, $[\text{E}_{14}]^{4-}$, $[\text{E}_{16}]^{2-}$,

$[\text{E}_{19}]^{3-}$, $[\text{E}_{21}]^{3-}$, $[\text{E}_{22}]^{4-}$, $[\text{E}_{26}]^{4-}$),¹ the most extensively studied are trianionic heptapnictide species, $[\text{Pn}_7]^{3-}$ ($\text{Pn} = \text{P}, \text{As}, \text{Sb}$), which are readily accessed by dissolution of Zintl phases of general formulae A_3Pn_7 ($\text{A} = \text{Li}-\text{Cs}$; $\text{Pn} = \text{P}-\text{Sb}$).² The missing member of this family, $[\text{Bi}_7]^{3-}$, previously unavailable due to the lack of a suitable A_3Bi_7 phase, was isolated by a solution-phase method by Sevov and co-workers earlier this year.³ The reactivity of this isostructural family has been irregularly studied, with the greatest attention being paid to the heptaphosphide trianion, $[\text{P}_7]^{3-}$, on account of its accessibility and the valuable spectroscopic information available through use of ^{31}P NMR spectroscopy. It has been empirically observed that while the lighter $[\text{Pn}_7]^{3-}$ anions tend to favour functionalization and/or coordination to transition metals (generally retaining their geometry and nuclearity),⁴ the heavier analogues can give rise to clusters of increased nuclearities on account of their weaker $\text{Pn}-\text{Pn}$ bonds.⁵ In recent years, however, it has been demonstrated that the metal-mediated activation of the lighter $[\text{P}_7]^{3-}$ and $[\text{As}_7]^{3-}$ cages is also a possibility.⁶

The $[\text{P}_7]^{3-}$ anion displays a nortricyclane-like structure and is both a strong reductant (readily being oxidized to higher nuclearity polyphosphides such as $[\text{P}_{16}]^{2-}$ and $[\text{P}_{21}]^{3-}$) and nucleophilic (as evidenced by its ability to afford $[\text{R}_x\text{P}_7]^{(3-x)-}$ ($x = 1-3$) type clusters).¹ Amongst the multitude of transformations available to $[\text{Pn}_7]^{3-}$ anions,¹ it has recently been shown that they are capable of heterolytically cleaving weak metal–carbon bonds in homoleptic organometallic species to afford heteroatomic clusters and *exo*-functionalized species.^{7–10} These anions are interesting not only for purely fundamental reasons, but also on account of their potential as precursors to novel cluster-assembled materials.¹¹

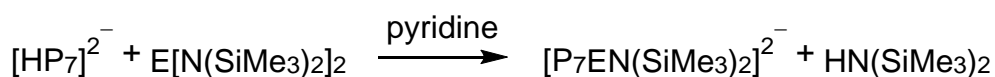
By contrast with the chemistry of $[\text{Pn}_7]^{3-}$ clusters, the chemistry of their protonated analogues, $[\text{HPn}_7]^{2-}$, is less developed, despite the fact that there is extensive literature

evidence that these species are often formed in the presence of trace amounts of moisture or in the presence of protic solvents. Despite being known for some time,¹² it was not until recently that preparative scale syntheses of $[\text{HPn}_7]^{2-}$ were reported by our research group.¹³ These species open up an interesting new avenue of exploration as they incorporate a weak Brønsted acidic site which may be used for the synthesis of new *exo*-functionalized cluster anions. Herein we describe the reactivity of $[\text{HP}_7]^{2-}$ towards homoleptic amides of the group 14 elements, $\text{E}[\text{N}(\text{SiMe}_3)_2]_2$ (E = Ge, Sn, Pb), and show that novel functionalized clusters are available accompanied by the formation of a stoichiometric amount of the amine $\text{HN}(\text{SiMe}_3)_2$.

2. Results and discussion

2.1. Synthesis and characterization of $[\text{P}_7\text{EN}(\text{SiMe}_3)_2]^{2-}$ (E = Ge (1), Sn (2) and Pb (3))

Reactions of $[\text{K}(18\text{-crown-6})][\text{HP}_7]$ (18-crown-6: 1,4,7,10,13,16-hexaoxacyclooctadecane) with the homoleptic group 14 amides $\text{E}[\text{N}(\text{SiMe}_3)_2]_2$ (E = Ge, Sn, Pb) in a 1:1 stoichiometric ratio (Scheme 1) were monitored by ^{31}P NMR spectroscopy revealing the quantitative transformation of $[\text{HP}_7]^{2-}$ into novel cluster anions with five magnetically inequivalent phosphorus environments. The ^1H NMR spectra of these reaction mixtures revealed the formation of free bis(trimethylsilyl)amine, $\text{HN}(\text{SiMe}_3)_2$, as a reaction side product as well as confirming the presence of an amide substituent on the *exo*-functionalized cages. This led us to hypothesise that the anions being formed bear a group 14 element amide substituent, i.e. $[\text{P}_7\text{EN}(\text{SiMe}_3)_2]^{2-}$ (E = Ge (1), Sn (2) and Pb (3)). This reactivity is consistent with our previous observation that deprotonation of $[\text{HP}_7]^{2-}$ to afford $[\text{P}_7]^{3-}$ is possible using $\text{K}[\text{N}(\text{SiMe}_3)_2]$.^{13b}



Scheme 1. Formation of $[\text{P}_7\text{EN}(\text{SiMe}_3)_2]^{2-}$ (E = Ge (1), Sn (2) and Pb (3)).

The ^{31}P NMR spectra of **1** and **2** are characteristic of κ^2 -coordination compounds of the $[\text{P}_7]^{3-}$ cage. They each reveal five resonances with relative intensities of 1:2:1:1:2. There is no significant change to the spectra on proton decoupling, which is consistent with the proposed deprotonation of the $[\text{HP}_7]^{2-}$ cage and concomitant formation of $\text{HN}(\text{SiMe}_3)_2$. The spectra for both compounds are very similar with minor changes to the chemical shifts of the coordinated cage. Resonances for **1** were observed at 72.3, 8.2, -46.2 , -61.0 and -189.5 ppm (Figure 1) and correspond to the P4, P2/P3, P1, P7 and P5/P6 nuclei, using the numbering scheme employed in Figure 2. The same resonances occur at 62.5, -18.1 , -38.7 , -81.4 and -192.0 ppm in the ^{31}P NMR spectrum of **2** and show comparable multiplet structures. Full tables of experimentally determined and computed coupling constants are provided in the Electronic Supplementary Material (ESI). The ^{119}Sn NMR spectrum of **2** reveals a singlet at -61.1 ppm consistent with the presence of a tin(II) amide functional group. The ^{29}Si NMR spectra for both clusters revealed the presence of trimethylsilyl groups, these were observed at -6.9 , -7.3 ppm for **1** and **2**, respectively

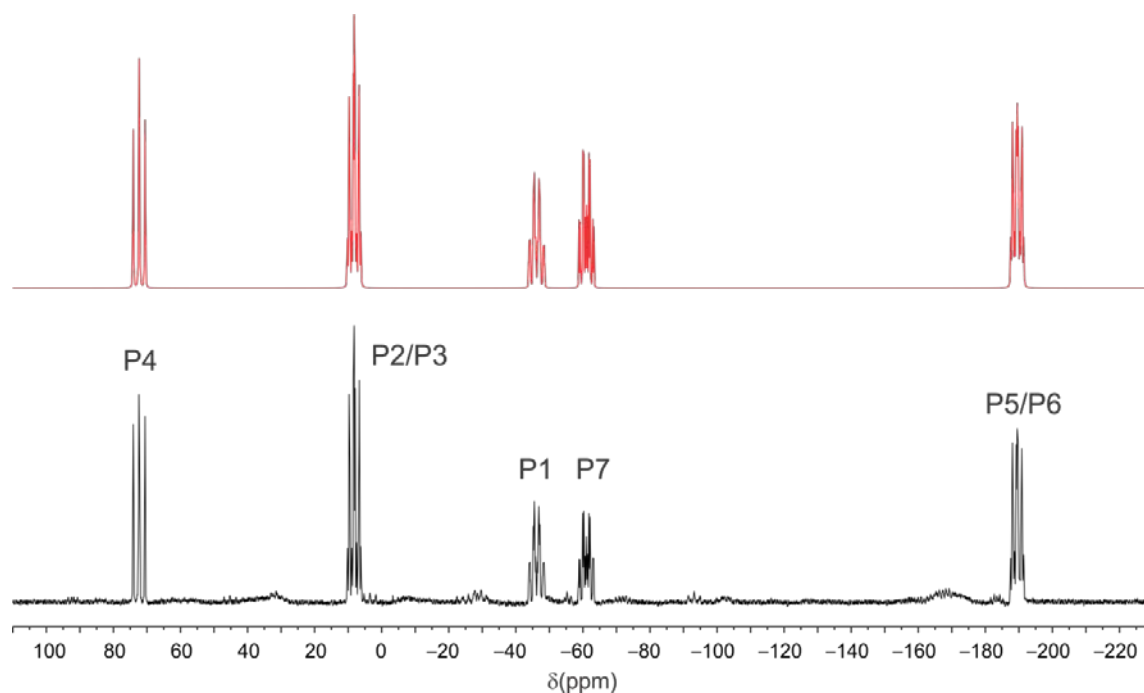


Figure 1: $^{31}\text{P}\{^1\text{H}\}$ NMR spectra for **1**. Top: simulated spectrum; bottom: recorded spectrum in d_5 -pyridine.

By contrast, the NMR data obtained for **3** were of much poorer quality, which is consistent with the extensive decomposition that was observed in the crude reaction mixtures. Despite this, however, five poorly resolved resonances of comparable chemical shifts to **1** and **2** were recorded in the ^{31}P NMR spectrum at 59.7, -17.2, -37.9, -84.5 and -197.5 ppm. However, due to the poor quality of the spectrum a suitable spectral simulation was not obtainable. A singlet was also observed in the ^{29}Si NMR spectrum of **3** at -7.1 ppm, which is in line with the values observed for **1** and **2**. It is reasonable to assume that **3** is formed in solution to some extent but rapidly decomposes to amorphous largely insoluble products we have yet to identify. Such decomposition precluded us from obtaining higher quality NMR spectra or a single crystal X-ray structure for the anion.

Further characterization of the cluster anions in solution was obtained by means of electrospray ionization mass spectrometry (ESI-MS). Negative ion mode mass spectra of **1** and **2** reveal the presence of the $[\text{P}_7\text{E}(\text{N}(\text{SiMe}_3)_2)]^-$ molecular ions at m/z values of 452.2 and 495.9, respectively. However, there is also evidence of extensive fragmentation during the ionisation process. The $[\text{P}_7\text{E}]^-$ ions were observed as the principal mass envelopes at 291.6 and 337.4 Da for **1** and **2**, respectively. Additionally, in the positive ion mode spectrum of solutions of **2**, $\{[\text{K}(\text{18-crown-6})]_3[\text{P}_7\text{SnN}(\text{SiMe}_3)_2]\}^+$ was observed at 1405.6 Da. The negative ion mode spectrum of the crude reaction mixtures that yielded **3** only revealed the presence of the $[\text{P}_7\text{Pb}]^-$ anion at 426.0 Da. Interestingly, and in contrast to what was observed for reactions with the lighter group 14 bisamides, a mass envelope corresponding to $[\text{P}_7(\text{SiMe}_3)_2]^-$ was also observed in the crude reaction mixture which afforded **3**.

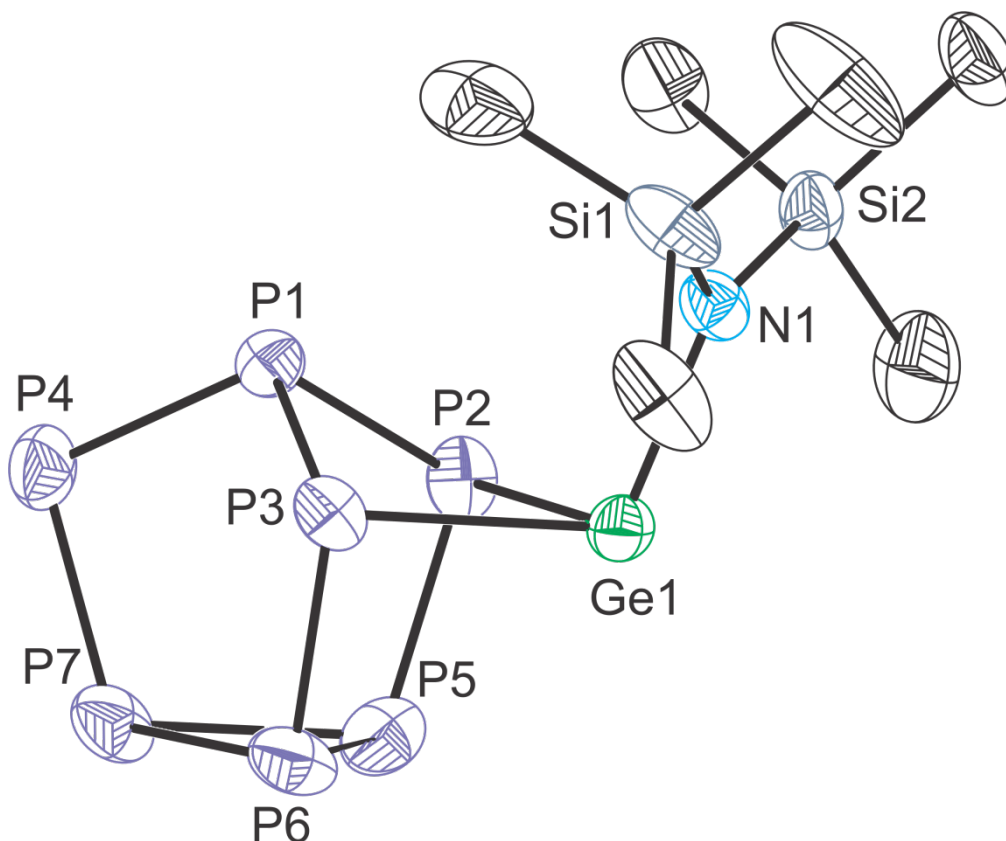


Figure 2. Molecular structure of the anionic moiety structurally characterized in $[\text{K}(\text{18-crown-6})]_2[\mathbf{1}] \cdot 2\text{py}$. Anisotropic thermal displacement ellipsoids are pictured at the 50% probability level. Hydrogen atoms have been removed for clarity. Selected interatomic distances (Å) and angles (°): P1–P2: 2.198(1); P1–P3: 2.196(1); P1–P4: 2.139(1); P2–P5: 2.178(1); P3–P6: 2.179(1); P4–P7: 2.148(1); P5–P6: 2.265(1); P5–P7: 2.235(1); 2.265(1); P6–P7: 2.234(1); P2–Ge1: 2.526(1); P3–Ge1: 2.504(1); Ge1–N1: 2.000(2); N1–Si1: 1.715(2); N1–Si2: 1.708(2); P2–Ge1–P3: 79.14(2); P2–Ge1–N1: 103.26(5); P3–Ge1–N1: 103.75(6).

The derivatized cluster anions **1** and **2** were further characterized crystallographically as $[\text{K}(\text{18-crown-6})]^+$ salts. It is worth noting that due to the instability of solutions of **1** at room temperature (*vide infra*), crystals were grown at $-35\text{ }^\circ\text{C}$ **over the course of a month**. Crystals of $[\text{K}(\text{18-crown-6})]_2[\mathbf{1}] \cdot 2\text{py}$ and $[\text{K}(\text{18-crown-6})]_2[\mathbf{2}] \cdot 2\text{py}$ are isomorphous, crystallizing in

the same space group ($P\bar{1}$; no. 2) with similar unit cell parameters. The structure of **1** is pictured in Figure 2, while the structure of **2** and a comparison of bond metric data for both species are provided in the ESI. Both dianions exhibit a $[\text{P}_7]^{3-}$ cage bonded in a κ^2 -fashion to a formally cationic $[\text{E}(\text{NSiMe}_3)]^+$ fragment. Bond metric data for the $[\text{P}_7]^{3-}$ cages are identical within experimental error and closely related to other structures exhibiting a similar coordination mode of the cage (such as, for example, $[\text{P}_7\text{In}(\text{C}_6\text{H}_5)_2]^{2-}$).⁷ There is a pyramidal arrangement around the group 14 element due to the presence of a stereogenic lone pair and consequently the sum of bond angles around E is notably less than 360° ($\Sigma_{\text{angles}} = 286.2^\circ$ for **1** and 279.0° for **2**). As would be expected the P–Ge bond lengths in **1** (2.526(1) and 2.504(1) Å) are on average 0.16 Å shorter than the P–Sn distances recorded for **2** (2.691(1) and 2.667(1) Å), which is fully consistent with the greater covalent radius of tin relative to germanium ($r_{\text{Sn}} - r_{\text{Ge}} = 0.19$ Å).¹⁴ Logically this has an effect on the P–E–P bond angle which is more acute for **2** than for **1** ($75.33(3)$ and $79.14(2)^\circ$, respectively).

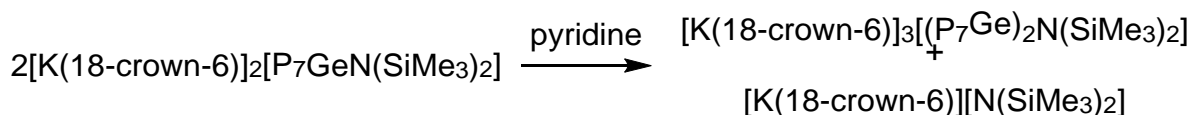
The computed geometries for **1** and **2** at the density functional level of theory (DFT) are in good agreement with the crystallographically determined structures (see ESI for full details). The computed structure of **3** also displays a comparable geometry with a pyramidal lead atom and suitable bond lengths and angles. As expected, the highest occupied molecular orbitals (HOMO) for **1** and **2** have a significant degree of orbital participation from the group 14 element (31.4 and 28.6%, respectively), with some mixing in of cluster-based and amide nitrogen orbitals. The analogous orbital for the lead-containing analogue, **3**, is the HOMO–1 which has a lesser degree of “lone-pair” character on the lead atom (15.7%) and a decreased participation of the more core-like 6s orbital. An analysis of computed Mulliken charges reveals significant negative charges on P2, P3 and P4 (using the numbering scheme employed in Figure 2) as well as on the amide nitrogen. All of the cluster phosphorus atoms carry some

degree of negative charge indicating charge delocalization throughout the cluster. Interestingly, the Mulliken charges on the group 14 elements increase on descending the group (−0.082, 0.189 and 0.423 for **1**, **2** and **3**, respectively), indicating that while formally the clusters can be interpreted as coordination complexes of a $[P_7]^{3-}$ cage with an $[EN(SiMe_3)_2]^+$ fragment, this formalism is only a good approximation for cluster **3**. The cluster anions of the lighter group 14 elements are probably best understood as systems where the tetrel elements are involved in more covalent interactions with the cluster (as opposed to acting as Lewis acids accepting electron density from the cluster cage). The greater participation of the lighter group 14 elements in cluster bonding may account for the relative instability of **1** in solution which was found to spontaneously give rise to a new cluster anion when left standing at room temperature.

2.2. Synthesis and characterization of $[(P_7Ge)_2N(SiMe_3)_2]^{3-}$ (**4**)

When a solution of **1** was left at room temperature for several days the ^{31}P NMR spectrum revealed quantitative conversion to a single species with seven inequivalent phosphorus environments (**4**). This process was observed repeatedly on a number of samples and can be indefinitely retarded by keeping solutions of **1** at low temperatures (−35 °C). The seven resulting ^{31}P NMR resonances were observed at 33.0, −25.8, −27.6, −70.7, −91.4, −165.9 and −182.1 ppm, with the two multiplets at −25.8 and −27.6 overlapping extensively (Figure 3). Attempts to crystallise this final product were entirely unsuccessful despite our effort to utilise a variety of solvents/anti-solvents and crystallization conditions. Similarly attempts to exchange the cation sequestering agent 18-crown-6 with 2,2,2-crypt (4,7,13,16,21,24-hexaoxa-1,10-diazabicyclo[8.8.8]hexacosane) in order to aid crystallization did not produce crystalline samples suitable for single crystal X-ray diffraction. ESI-MS studies on these crude reaction mixtures show the presence of a mass envelope at 741.3 Da which is consistent with the

formation of $[(P_7Ge_2)_2N(SiMe_3)_2]^-$. These studies suggest that **1** dimerises in solution over prolonged periods of time with concomitant loss of an amide substituent (Scheme 2). This was confirmed by 1H and ^{29}Si NMR experiments which showed evidence for the formation of $[N(SiMe_3)_2]^-$.



Scheme 2. Formation of $[(P_7Ge_2)_2N(SiMe_3)_2]^{3-}$ (**4**) from $[P_7GeN(SiMe_3)_2]^{2-}$ (**1**).

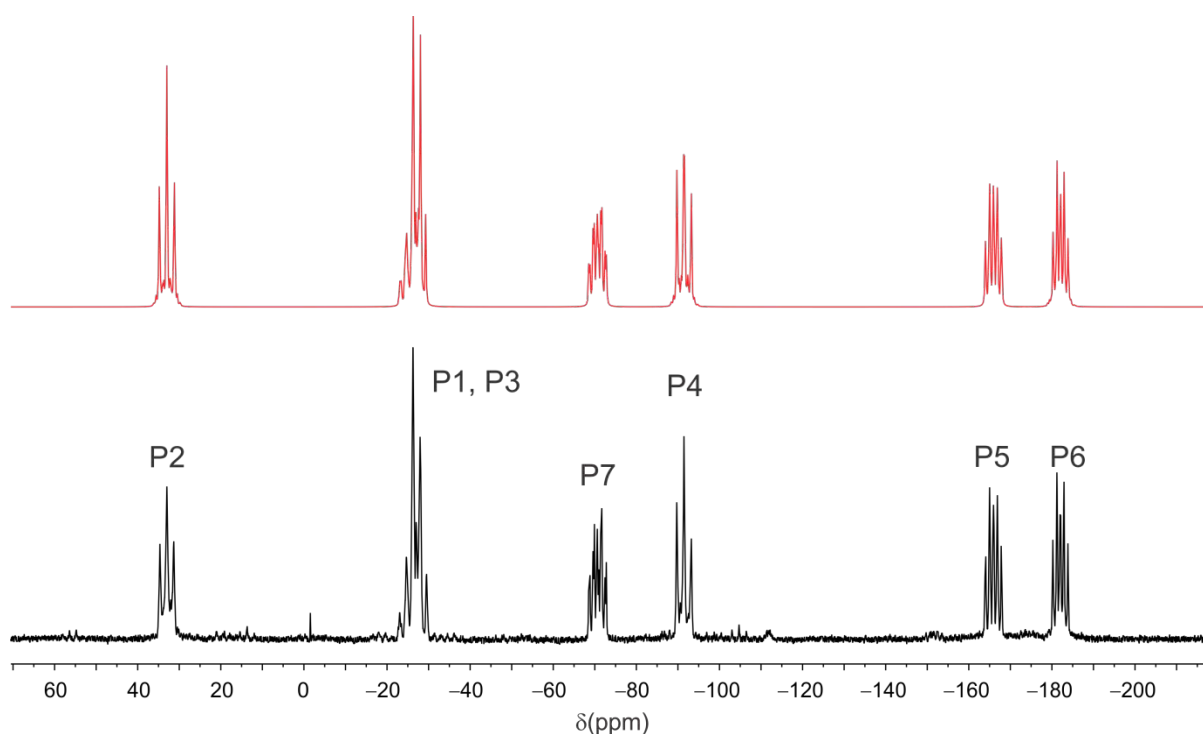


Figure 3: $^{31}P\{^1H\}$ NMR spectra for **4**. Top: simulated spectrum; bottom: recorded spectrum in d_5 -pyridine.

This failure to obtain crystalline samples of **4** led us to attempt the *in situ* generation of a precursor of nominal formula $[K(15\text{-crown-5})_2]_2[HP_7]$ by reaction of K_3P_7 with six equivalents of 15-crown-5 and stoichiometric amounts of water. Addition of one equivalent

of $\text{Ge}[\text{N}(\text{SiMe}_3)_2]_2$ to this mixture revealed an identical ^{31}P NMR spectrum to those obtained when carrying out the same reaction with $[\text{K}(18\text{-crown-6})]_2[\text{HP}_7]$. Initial formation of **1** ultimately gives rise to **4** over the course of three days when the mixture is kept at room temperature (five resonances were observed in the ^{31}P NMR spectrum of the mixture at 31.3, -27.2, -29.3, -70.9, -92.3, -164.9 and -182.4 ppm). From these reactions, crystalline samples can be obtained, which when analysed by single crystal X-ray diffraction, allowed us to determine the connectivity and composition of the resulting product: $[\text{K}(15\text{-crown-5})_2]_3[(\text{P}_7\text{Ge})_2\text{N}(\text{SiMe}_3)_2] \cdot x(\text{solv})$.¹⁵ It is worth noting however, that the quality of the crystal structure obtained is very poor due to extensive disorder of the 15-crown-5 moieties in the lattice and a satisfactory solution could not be obtained. Nevertheless, the partial structure permitted us to determine the structure of the anionic moiety, $[(\text{P}_7\text{Ge})_2\text{N}(\text{SiMe}_3)_2]^{3-}$ (**4**), and locate the K^+ cations. This, in turn, allowed for the simulation of the ^{31}P NMR spectrum obtained for **4**.

The structure of **4** (Figure 4) is related to that of the well-known polyphosphide $[\text{P}_{16}]^{2-}$. This is perhaps unsurprising as both systems are isoelectronic. The replacement of two bridging three-connect phosphorus atoms in $[\text{P}_{16}]^{2-}$ with a $\text{GeN}(\text{SiMe}_3)_2$ moiety and a substituent-free germanium atom gives rise to an increase in the overall negative charge of the anion (P is isoelectronic with GeR or Ge^+). Related substituted clusters, $[\text{EP}_{15}]^{3-}$ ($\text{E} = \text{Sn}, \text{Pb}$) and $[\text{SnAs}_{15}]^{3-}$, have previously been reported by our research group and exhibit comparable structures.^{4k} Due to the poor quality of the crystalline samples obtained, the structure is unsuitable for the discussion of bond metric data, however the connectivity and general geometry of the anion is unambiguous. The structure as determined by X-ray diffraction was computed using DFT methods converging to give a stable trianionic species which is in good

agreement with the X-ray data obtained. DFT calculations also afforded coupling constant data for **4** which correlate with the simulated ^{31}P NMR spectrum (see ESI for full details).

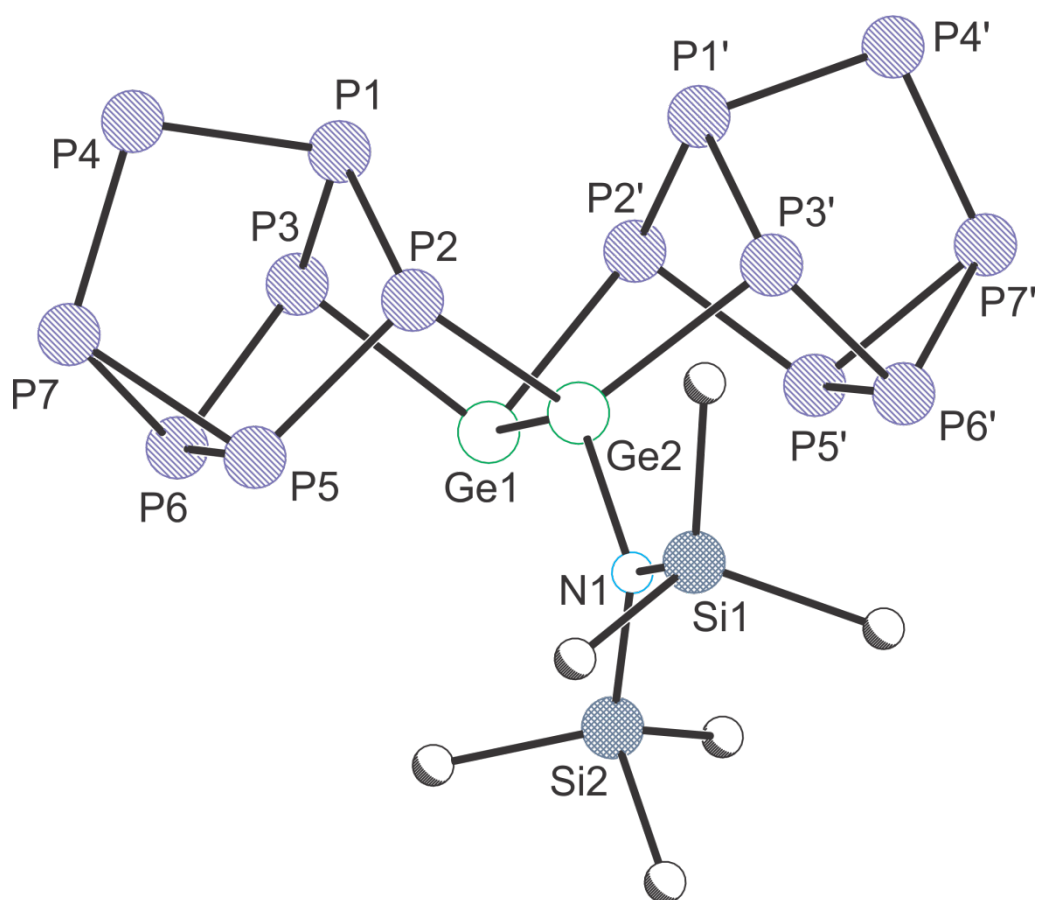


Figure 4. Ball-and-stick molecular structure representation of the anionic moiety structurally characterized in $[\text{K}(\text{15-crown-5})_2][\mathbf{4}] \cdot x(\text{solv})$. Symmetry operation $'$: $x, 0.5-y, z$.

The thermodynamic instability of **1** in solution was probed using DFT computational methods. The decomposition of two molecules of **1** to give rise to **4** and one equivalent of bis(trimethylsilyl)amide, $[\text{N}(\text{SiMe}_3)_2]^-$, was found to be thermodynamically favourable by $20.43 \text{ kJ mol}^{-1}$. This value is the result of arithmetically combining the computed total bonding energies obtained for the optimized structures of the systems in question (*i.e.* $2(-17984.07) - (-22217.17 - 13771.40) = 20.43 \text{ kJ mol}^{-1}$). By contrast, recombination of two molecules of **2** to afford the unobserved compound $[(\text{P}_7\text{Sn}_2)_2\text{N}(\text{SiMe}_3)_2]^{3-}$ (**5**) and $[\text{N}(\text{SiMe}_3)_2]^-$ is thermodynamically uphill by 27.5 kJ mol^{-1} . These values are consistent with

the observation that **1** readily affords **4** over time, whereas solutions of **2** are indefinitely stable.

3. Conclusions

We have shown that the protonated heptaphosphide dianion, $[\text{HP}_7]^{2-}$, reacts with one equivalent of $\text{E}[\text{N}(\text{SiMe}_3)_2]_2$ ($\text{E} = \text{Ge}, \text{Sn}, \text{Pb}$) to give rise to novel derivatized cluster anions $[\text{P}_7\text{EN}(\text{SiMe}_3)_2]^{2-}$ ($\text{E} = \text{Ge}$ (**1**), Sn (**2**) and Pb (**3**)). The thermodynamic stability of these species was found to vary significantly depending on the nature of the group 14 element in question. Thus while **1** was found to be unstable in solution over the course of days (ultimately affording $[(\text{P}_7\text{Ge}_2)_2\text{N}(\text{SiMe}_3)_2]^{3-}$ (**4**)), solutions of **2** are indefinitely stable (these observations are supported by DFT level calculations). The decomposition of **1** over time offers some insight into how other related (and unusual) higher nuclearity polyphosphides such as $[\text{EP}_{15}]^{3-}$ ($\text{E} = \text{Sn}, \text{Pb}$) and $[\text{SnAs}_{15}]^{3-}$ may be formed, and strongly suggests the formation of intermediates consisting of the seven-membered $[\text{P}_7]^{3-}$ cage.

4. Experimental

General synthetic methods. All reactions and product manipulations were carried out under an inert atmosphere of argon or dinitrogen using standard Schlenk-line or glovebox techniques (MBraun UNIlab glovebox maintained at < 0.1 ppm H_2O and < 0.1 ppm O_2). K_3P_7 was synthesized according to a previously reported synthetic procedure from a mixture of the elements (K : 99.95%, Strem; P : 99.99%, Sigma-Aldrich) heated to 700°C for 60 h in sealed niobium containers (jacketed inside a flame-sealed silica ampoule under vacuum in order to avoid oxidation of the niobium vessels).^{2e} $[\text{K}(18\text{-crown-6})][\text{HP}_7]$ was prepared according to a previously reported synthetic procedure.¹³ $\text{E}[\text{N}(\text{SiMe}_3)_2]_2$ ($\text{E} = \text{Ge}, \text{Pb}$) were synthesized as previously reported by Lappert and co-workers while $\text{Sn}[\text{N}(\text{SiMe}_3)_2]_2$ (98%, Sigma-Aldrich)

was purchased commercially and used as received.¹⁶ 18-crown-6 (1,4,7,10,13,16-hexaoxacyclooctadecane; 99%, Alfa-Aesar) was used as received after careful drying under vacuum. Toluene (tol; HPLC grade, Sigma-Aldrich), Et₂O (Pesticide residue grade, Fisher) and dimethylformamide (DMF; 99.9%, Rathburn) were purified using an MBraun SPS-800 solvent system. Pyridine (py; 99+%, Alfa Aesar) and *d*₅-pyridine (99.5%, Cambridge Isotope Laboratories) were distilled over CaH₂. All dry solvents were stored under argon in gas-tight ampoules. Additionally toluene was stored over activated 3 Å molecular sieves.

[K(18-crown-6)]₂[P₇GeN(SiMe₃)₂]₂·2py ([K(18-crown-6)]₂[**1**]₂·2py). Ge[N(SiMe₃)₂]₂ (38 mg, 0.10 mmol) and [K(18-crown-6)]₂[HP₇] (80 mg, 0.14 mmol) were dissolved in pyridine (1 mL) yielding a light orange solution. The solution was filtered and light-orange block-like crystals of [K(18-crown-6)]₂[P₇GeN(SiMe₃)₂]₂·2py were grown by vapour diffusion of toluene into a very concentrated pyridine solution at –35 °C over the course of a month. Crystalline yield: 12 mg (9%). CCDC 1408315. A suitable elemental analysis could not be obtained due to the inherent instability of the anion (*vide infra*). ¹H NMR (500 MHz, *d*₅-pyridine, 298 K): δ (ppm) 3.56 (24H, s, 18-crown-6), 0.87 (18H, s, [P₇GeN(SiMe₃)₂]^{2–}). ³¹P{¹H} NMR (202.4 MHz, *d*₅-pyridine, 298 K): δ (ppm) 72.3 (1P, m; P₄), 8.2 (2P, m; P₂/P₃), –46.2 (1P, m; P₁), –61.0 (1P, m; P₇), –189.5 (1P, m; P₅/P₆). ¹³C{¹H} NMR (125.8 MHz, *d*₅-pyridine, 298 K): δ (ppm) 71.0 (18-crown-6), 7.9 ([P₇GeN(SiMe₃)₂]^{2–}). ²⁹Si NMR (99.32 MHz, *d*₅-pyridine, 298 K): δ (ppm) –6.9 (s, P₇Ge[N(SiMe₃)₂][–]). ESI-MS (–ve ion mode, DMF): *m/z* 216.5 (98%) [P₇][–], 291.6 (100%) [P₇Ge][–], 452.2 (43%) [P₇Ge(N(SiMe₃)₂)][–].

[K(18-crown-6)]₂[P₇SnN(SiMe₃)₂]₂·2py ([K(18-crown-6)]₂[**2**]₂·2py). Sn[N(SiMe₃)₂]₂ (60 mg, 0.14 mmol) and [K(18-crown-6)]₂[HP₇] (112 mg, 0.14 mmol) were dissolved in pyridine (1 mL) yielding an orange solution. The reaction mixture was stirred for 5 min. Following

filtration, orange block-like crystals of $[\text{K}(\text{18-crown-6})]_2[\text{P}_7\text{SnN}(\text{SiMe}_3)_2]\cdot 2\text{py}$ were grown by vapour diffusion of toluene into a concentrated pyridine solution. Crystalline yield: 132 mg (76%). CCDC 1408315. Anal. calcd. for $[\text{K}(\text{18-crown-6})]_2[\text{P}_7\text{SnN}(\text{SiMe}_3)_2]$ ($\text{C}_{30}\text{H}_{66}\text{K}_2\text{NO}_{12}\text{P}_7\text{Si}_2\text{Sn}$; $1102.46 \text{ g mol}^{-1}$): C 32.68, H 6.03, N 1.27. Found: C 32.14, H 5.67, N 1.46. ^1H NMR (500 MHz, d_5 -pyridine, 298 K): δ (ppm) 3.51 (24H, s; 18-crown-6), 0.85 (18H, s; $[\text{P}_7\text{Sn}(\text{N}(\text{SiMe}_3)_2)]^{2-}$). $^{31}\text{P}\{^1\text{H}\}$ NMR (202.4 MHz, d_5 -pyridine, 298 K): δ (ppm) 62.5 (1P, t; P4), -18.1 (2P, m; P2/P3), -38.7 (1P, m; P1), -81.4 (1P, m; P7), -192.0 (1P, t; P5/P6). $^{13}\text{C}\{^1\text{H}\}$ NMR (125.8 MHz, d_5 -pyridine): δ (ppm) 71.0 (18-crown-6), 8.02 ($[\text{P}_7\text{Sn}(\text{N}(\text{SiMe}_3)_2)]^{2-}$). ^{119}Sn NMR (186.43 MHz, d_5 -pyridine, 298 K): δ (ppm) -61.1 (s, $[\text{P}_7\text{Sn}(\text{N}(\text{SiMe}_3)_2)]^{2-}$). ^{29}Si NMR (99.32 MHz, d_5 -pyridine, 298 K): δ (ppm) -7.3 (s, $\text{P}_7\text{Sn}[\text{N}(\text{SiMe}_3)_2]^-$). ESI-MS (-ve ion mode; DMF): m/z 337.4 (100%) $[\text{P}_7\text{Sn}]^-$, 495.9 (15%) $[\text{P}_7\text{Sn}(\text{N}(\text{SiMe}_3)_2)]^-$. ESI-MS (+ve ion mode; DMF): m/z 1405.6 $\{[\text{K}(\text{18-crown-6})]_3[\text{P}_7\text{Sn}(\text{N}(\text{SiMe}_3)_2)]\}^+$.

$[\text{K}(\text{18-crown-6})]_2[\text{P}_7\text{PbN}(\text{SiMe}_3)_2]$ ($[\text{K}(\text{18-crown-6})]_2[\mathbf{3}]$). $\text{Pb}[\text{N}(\text{SiMe}_3)_2]_2$ (44 mg, 0.09 mmol) and $[\text{K}(\text{18-crown-6})]_2[\text{HP}_7]$ (70 mg, 0.09 mmol) were dissolved pyridine (1 mL) yielding a dark red solution. After stirring the reaction mixture for 30 minutes, the resulting solution was filtered. Despite numerous attempts, single crystals of the product could not be grown. Due to the lack of a compositionally pure product a suitable elemental analysis was not obtained. ^1H NMR (499.93 MHz, d_5 -pyridine, 298 K): δ (ppm) 3.54 (24H, s; 18-crown-6), 0.81 (18H, s; $[\text{P}_7\text{Sn}(\text{N}(\text{SiMe}_3)_2)]^{2-}$). $^{31}\text{P}\{^1\text{H}\}$ NMR (161.98 MHz, d_5 -pyridine, 298 K): δ (ppm) 59.7 (1P, m; P4), -17.2 (2P, broad m; P2/P3), -37.9 (1P, broad m; P1), -84.5 (1P, broad m; P7), -197.5 (2P, broad s; P5/P6). $^{13}\text{C}\{^1\text{H}\}$ NMR (125.8 MHz, d_5 -pyridine, 298 K): δ (ppm) 70.9 (18-crown-6), 8.13 ($[\text{P}_7\text{Pb}(\text{N}(\text{SiMe}_3)_2)]^{2-}$). ^{29}Si NMR (99.32 MHz, d_5 -pyridine): δ

(ppm) -7.1 (s, $[\text{P}_7\text{PbN}(\text{SiMe}_3)_2]^-$). ESI-MS (–ve ion mode, DMF): m/z 217.7 (100%) $[\text{HP}_7]^-$, 288.9 (20%) $[\text{P}_7(\text{SiMe}_3)]^-$, 360.1 (100%) $[\text{P}_7(\text{SiMe}_3)_2]^-$, 426.0 (70%) $[\text{P}_7\text{Pb}]^-$.

$[\text{K}(\text{15-crown-5})]_3[(\text{P}_7)_2\text{Ge}_2\text{N}(\text{SiMe}_3)_2]$ ($[\text{K}(\text{15-crown-5})]_3[\mathbf{4}]$).

$\text{Ge}[\text{N}(\text{SiMe}_3)_2]_2$ (66 mg, 0.17 mmol) and $[\text{K}(\text{15-crown-5})_2]_2[\text{HP}_7]$ (198 mg, 0.17 mmol) were dissolved in pyridine (2 mL) yielding a light orange solution. The reaction mixture was then monitored by ^{31}P NMR spectroscopy for a 90 h period and a gradual colour change from light orange to red was observed. All volatiles were removed under vacuum and the resulting orange oil was washed with diethyl ether (10 mL) to give rise to an orange powder. The orange powder was dissolved in pyridine and filtered into an airtight ampoule. Slow diffusion of diethyl ether into the pyridine solution afforded orange needles suitable for X-ray diffraction after three days. Yield 130 mg (94%). Anal. calcd. for $[\text{K}(\text{15-crown-5})_2]_3[(\text{P}_7)_2\text{Ge}_2\text{N}(\text{SiMe}_3)_2]$ ($\text{C}_{66}\text{H}_{138}\text{Ge}_2\text{K}_3\text{NO}_{30}\text{P}_{14}\text{Si}_2$; $2177.8 \text{ g mol}^{-1}$): C 36.40, H 6.39, N 0.64. Found: C 36.5, H 6.25, N 0.96. ^1H NMR (500 MHz, d_5 -pyridine, 298 K): δ (ppm) 3.61 (s, 40H; 15-crown-5), 1.08 (s, 18H; $[(\text{P}_7\text{Ge})_2\text{N}(\text{SiMe}_3)_2]^{3-}$). $^{31}\text{P}\{^1\text{H}\}$ NMR (202.4 MHz, d_5 -pyridine, 298 K): δ (ppm) 31.3 (t, 1P; P2), -27.2 (m overlapping, 1P; P1), -29.3 (m overlapping, 1P; P3), -70.9 (m, 1P; P7), -92.3 (m, 1P; P4), -164.9 (t, 1P; P5), -182.4 (m, 1P; P6). $^{13}\text{C}\{^1\text{H}\}$ NMR (125.8 MHz, d_5 -pyridine, 298 K): δ (ppm) 69.4 (15-crown-5), 16.0 $[(\text{P}_7\text{Ge})_2\text{N}(\text{SiMe}_3)_2]$. ^{29}Si NMR (99.32 MHz, d_5 -pyridine, 298 K): δ (ppm) 2.5 (s, $[(\text{P}_7\text{Ge})_2\text{N}(\text{SiMe}_3)_2]$). ESI-MS (–ve ion mode, DMF): m/z 216.5 (100%) $[\text{P}_7]^-$, 291.6 (99%) $[\text{P}_7\text{Ge}]^-$, 741.3 (70%) $[(\text{P}_7\text{Ge})_2\text{N}(\text{SiMe}_3)_2]^-$.

Characterization techniques. Single crystal X-ray diffraction data were collected using an Enraf-Nonius kappa-CCD diffractometer equipped with a 95 mm CCD area detector. Crystals were selected under Paratone-N oil, mounted on micromount loops and quench-cooled using an Oxford Cryosystems open flow N_2 cooling device.¹⁷ Data were collected at 150 K using

graphite monochromated Mo K_{α} radiation ($\lambda = 0.71073 \text{ \AA}$). Equivalent reflections were merged and processed using the DENZO-SMN package, including unit cell parameter refinement and inter-frame scaling (which was carried out using SCALEPACK).¹⁸ Structures were subsequently solved using direct methods and refined on F^2 using the SHELXL 13-4 package.¹⁹

^1H , ^{13}C , ^{29}Si , ^{31}P and ^{119}Sn NMR spectra were acquired at 500.0, 125.8, 99.32, 202.4 and 186.43 MHz, respectively, on a Bruker AVIII 500 MHz NMR spectrometer. ^1H and ^{13}C NMR spectra were referenced to the most downfield residual solvent resonance (d_5 -pyridine: $\delta_{\text{H}} = 8.74 \text{ ppm}$, $\delta_{\text{C}} = 150.4 \text{ ppm}$ relative to $\text{Si}(\text{CH}_3)_4$ ($\delta = 0 \text{ ppm}$)). ^{29}Si , ^{31}P and ^{119}Sn spectra were externally referenced to $\text{Si}(\text{CH}_3)_4$ ($\delta_{\text{Si}} = 0 \text{ ppm}$), 85% H_3PO_4 ($\delta_{\text{P}} = 0 \text{ ppm}$) and SnMe_4 ($\delta_{\text{Sn}} = 0 \text{ ppm}$), respectively. All spectra were recorded at 25 °C. Spectral simulations were carried out using the gNMR v5.0 program²⁰. Data were processed using the Bruker TopSpin 3.2 program.

Elemental analyses were performed by Elemental Microanalysis Ltd., Devon. 5–10 mg samples were sent in sealed, evacuated Pyrex ampoules.

Table S1. Selected X-ray data collection and refinement parameters for [K(18-crown-6)]₂[**1**]·2py and [K(18-crown-6)]₂[**2**]·2py.

	[K(18-crown-6)] ₂ [1]·2py	[K(18-crown-6)] ₂ [2]·2py
Formula	C ₄₀ H ₇₆ GeK ₂ N ₃ O ₁₂ P ₇ Si ₂	C ₄₀ H ₇₆ K ₂ N ₃ O ₁₂ P ₇ Si ₂ Sn
Fw [g mol ⁻¹]	1214.79	1260.89
crystal system	triclinic	triclinic
space group	<i>P</i> −1	<i>P</i> −1
<i>a</i> (Å)	13.0810(2)	13.1078(2)
<i>b</i> (Å)	15.6526(3)	15.7005(2)
<i>c</i> (Å)	15.7164(3)	15.9468(3)
α (°)	87.749(1)	88.958(1)
β (°)	72.748(1)	72.667(1)
γ (°)	77.053(1)	77.311(1)
<i>V</i> (Å ³)	2993.78(10)	3052.36(9)
<i>Z</i>	2	2
radiation, λ (Å)	Mo K α , 0.71073	Mo K α , 0.71073
<i>T</i> (K)	150(2)	150(2)

ρ_{calc} (g cm ⁻³)	1.348	1.372
μ (mm ⁻¹)	0.930	0.829
reflections collected	23615	23003
independent reflections	13670	13918
parameters	791	738
R(int)	0.0215	0.0272
R1/wR2, ^[a] I $\geq 2\sigma_I$ (%)	3.93/9.55	4.96/11.99
R1/wR2, ^[a] all data (%)	5.76/10.57	7.70/13.52
GOF	1.006	0.974

^[a] $R1 = [\Sigma||F_o| - |F_c||]/\Sigma|F_o|$; $wR2 = \{[\Sigma w[(F_o)^2 - (F_c)^2]^2]/[\Sigma w(F_o^2)^2]\}^{1/2}$; $w = [\sigma^2(F_o)^2 + (AP)^2 + BP]^{-1}$, where $P = [(F_o)^2 + 2(F_c)^2]/3$ and the A and

B values are 0.0526 and 1.27 for [K(18-crown-6)]₂[**1**]·2py and 0.0615 and 4.84 for [K(18-crown-6)]₂[**2**]·2py.

5. Acknowledgement

We thank the Mexican Consejo Nacional de Ciencia y Tecnología (CONACyT; studentship GEQ) and the University of Oxford for financial support of this research. We also thank the University of Oxford for access to Chemical Crystallography and Advanced Research Computing (ARC) facilities.

6. References

- (1) For recent reviews see: (a) S. Scharfe, F. Kraus, S. Stegmaier, A. Schier and T. F. Fässler, *Angew. Chem. Int. Ed.*, 2011, **50**, 3630; (b) T. F. Fässler, *Struct. Bond.*, 2011, **140**, 91; (c) R. S. P. Turbervill and J. M. Goicoechea, *Chem. Rev.*, 2014, **114**, 10807.
- (2) (a) F. W. Dorn and W. Klemm, *Z. Anorg. Allg. Chem.*, 1961, **309**, 189; (b) W. Dahlmann and H. G. von Schnering, *Naturwissenschaften*, 1972, **59**, 420, (c) W. Dahlmann and H. G. von Schnering, *Naturwissenschaften*, 1973, **60**, 429; (d) W. Schmettow and H. G. von Schnering, *Angew. Chem. Int. Ed. Engl.*, 1977, **16**, 857; (e) V. Manriquez, W. Höhle and H. G. von Schnering, *Z. Anorg. Allg. Chem.*, 1986, **539**, 95; (f) R. P. Santandrea, C. Mensing, and H. G. von Schnering, *Thermochim. Acta*, 1986, **98**, 301; (g) T. Meyer, W. Höhle and H. G. von Schnering, *Z. Anorg. Allg. Chem.*, 1987, **552**, 69; (h) C. Hirschle and C. Röhr, *C. Z. Anorg. Allg. Chem.*, 2000, **626**, 1992; (i) W. Höhle, J. Buresch, K. Peters, J. H. Chang and H. von Schnering, *Z. Kristallogr. NCS*, 2002, **217**, 485; (j) W. Höhle, J. Buresch, K. Peters, J. H. Chang and H. von Schnering, *Z. Kristallogr. NCS*, 2002, **217**, 487. (k) W. Höhle, J. Buresch, J. Wolf, K. Peters, J. H. Chang and H. von Schnering, *Z. Kristallogr. NCS*, 2002, **217**, 489;
- (l) F. Emmerling and C. Röhr, *Z. Naturforsch.*, 2002, **57b**, 963.
- (3) L. G. Perla, A. G. Oliver and S. C. Sevov, *Inorg. Chem.*, 2015, **54**, 872.
- (4) For selected examples of $[E_7]^{3-}$ cluster anions coordinating to transition metals see: (a) B. W. Eichhorn, R. C. Haushalter and J. C. Huffman, *Angew. Chem. Int. Ed. Engl.*, 1989, **28**,

1032; (b) S. Charles, B. W. Eichhorn, A. L. Rheingold and S. G. Bott, *J. Am. Chem. Soc.*, 1994, **116**, 8077; (c) U. Bolle and W. Tremel, *J. Chem. Soc., Chem. Commun.*, 1994, 217; (d) S. Charles, J. C. Fetting, S. G. Bott and B. W. Eichhorn, *J. Am. Chem. Soc.*, 1996, **118**, 4713; (e) S. Charles, J. C. Fetting and B. W. Eichhorn, *Inorg. Chem.*, 1996, **35**, 1540; (f) S. Charles, J. A. Danis, J. C. Fetting and B. W. Eichhorn, *Inorg. Chem.*, 1997, **36**, 3772; (g) S. Charles, J. A. Danis, S. P. Mattamana, J. C. Fetting and B. W. Eichhorn, *Z. Anorg. Allg. Chem.*, 1998, **624**, 823; (h) B. Kesanli, S. Charles, Y.-F. Lam, S. G. Bott, J. Fetting and B. Eichhorn, *J. Am. Chem. Soc.*, 2000, **122**, 11101; (i) B. Kesanli, S. P. Mattamana, J. Danis and B. Eichhorn, *Inorg. Chim. Acta.*, 2005, **358**, 3145; (j) N. K. Chaki, S. Mandal, A. C. Reber, M. Qian, H. M. Saavedra, P. S. Weiss, S. N. Khanna, and A. Sen, *ACS Nano*, 2010, **4**, 5813; (k) C. M. Knapp, J. S. Large, N. H. Rees and J. M. Goicoechea, *Dalton Trans.*, 2011, **40**, 735; (l) C. M. Knapp, C. S. Jackson, J. S. Large, A. L. Thompson and J. M. Goicoechea, *Inorg. Chem.*, 2011, **50**, 4021; (m) C. M. Knapp, J. S. Large, N. H. Rees and J. M. Goicoechea, *Chem. Commun.*, 2011, **47**, 4111.

(5) For examples of the metal-mediated activation of $[E_7]^{3-}$ cluster anions see: (a) H. G. von Schnering, J. Wolf, D. Weber, R. Ramirez and T. Meyer, *Angew. Chem. Int. Ed. Engl.*, 1986, **25**, 353; (b) R. Ahlrichs, D. Fenske, K. Fromm, H. Krautscheid, U. Krautscheid and O. Treutler, *Chem. Eur. J.*, 1996, **2**, 238; (c) B. W. Eichhorn, S. P. Mattamana, D. R. Gardner, J. C. Fetting, *J. Am. Chem. Soc.*, 1998, **120**, 9708; (d) M. J. Moses, J. Fetting and B. Eichhorn, *J. Am. Chem. Soc.*, 2002, **124**, 5944; (e) B. Kesanli, J. Fetting and B. Eichhorn, *J. Am. Chem. Soc.*, 2003, **125**, 7367; (f) B. Kesanli, J. Fetting, B. Scott and B. Eichhorn, *Inorg. Chem.*, 2004, **43**, 3840; (g) J. Li and K. Wu, *Inorg. Chem.*, 2000, **39**, 1538; (h) M. J. Moses; J. C. Fetting and B. W. Eichhorn, *Science*, 2003, **300**, 778; (i) M. J. Moses, J. C. Fetting and B. W. Eichhorn, *Inorg. Chem.*, 2007, **46**, 1036.

- (6) (a) C. M. Knapp, B. H. Westcott, M. A. C. Raybould, J. E. McGrady and J. M. Goicoechea, *Angew. Chem., Int. Ed.*, 2012, **51**, 9097; (b) C. M. Knapp, B. H. Westcott, M. A. C. Raybould, J. E. McGrady and J. M. Goicoechea, *Chem. Commun.*, 2012, 48, 12183.
- (7) C. Knapp, B. Zhou, M. S. Denning, N. H. Rees and J. M. Goicoechea, *Dalton Trans.*, 2010, **39**, 426.
- (8) M. Qian, A. C. Reber, A. Ugrinov, N. K. Chaki, S. Mandal, H. M. Saavedra, S. N. Khanna, A. Sen, and P. S. Weiss, *ACS Nano*, 2010, **4**, 235.
- (9) S. Mandal, A. C. Reber, M. Qian, R. Liu, H. M. Saavedra, S. Sen, P. S. Weiss, S. N. Khanna and A. Sen, *Dalton Trans.*, 2012, **41**, 12365.
- (10) S. Mandal, A. C. Reber, M. Qian, R. Liu, H. M. Saavedra, S. Sen, P. S. Weiss, S. N. Khanna and A. Sen, *Dalton Trans.* 2012, **41**, 5454.
- (11) S. A. Claridge, A. W. Castleman Jr., S. N. Khanna, C. B. Murray, A. Sen and P. S. Weiss, *ACS Nano*, 2009, **3**, 244.
- (12) (a) M. Baudler, R. Heumüller and K. Langerbeins, *Anorg. Allg. Chem.*, 1984, **514**, 7; (b) J. C. Aschenbrenner and N. Korber, *Z. Anorg. Allg. Chem.*, 2004, **630**, 31; (c) F.-R. Dai, and L. Xu, *Inorg. Chim. Acta.*, 2006, **359**, 4265.
- (13) (a) R. S. P. Turbervill and J. M. Goicoechea, *Organometallics*, 2012, **31**, 2452; (b) R. S. P. Turbervill and J. M. Goicoechea, *Eur. J. Inorg. Chem.*, 2014, 1660.
- (14) (a) B. Cordero, V. Gómez, A. E. Platero-Prats, M. Revés, J. Echeverría, E. Cremades, F. Barragán and S. Alvarez, *Dalton Trans.*, 2008, 2832; (b) P. Pyykkö, M. Atsumi, *Chem. Eur. J.*, 2009, **15**, 186.
- (15) The sample crystallises in space group *Pnma* (no. 62) with the following unit cell parameters: $a = 29.2916(10) \text{ \AA}$, $b = 15.3280(6) \text{ \AA}$, $c = 27.2246(7) \text{ \AA}$; $V = 12223.3(7) \text{ \AA}^3$.
- (16) R. W. Chorley, P. B. Hitchcock, M. F. Lappert, W.-P. Leung, P. P. Power and M. M. Olmstead, *Inorg. Chim. Acta*, 1992, **198–200**, 203.

- (17) J. Cosier and A. M. Glazer, *J. Appl. Crystallogr.*, 1986, 105.
- (18) Z. Otwinowski and W. Minor, W., *Macromol. Crystallogr. Part A*, 1997, **276**, 307.
- (19) (a) G. M. Sheldrick, *SHELXL97, Programs for Crystal Structure Analysis (Release 97-2)* 1998; (b) G. M. Sheldrick, *Acta Crystallogr. Sect. A.*, 1990, **46**, 467; (c) G. M. Sheldrick, *Acta Crystallogr. Sect. A.*, 2008, **64**, 112.
- (20) gNMR v5.0, Budzelaar, P. H. M., 1995-2006, IvorySoft.

TOC

